Dynamic response of seismically isolated rigid blocks under near-fault ground motions

P.C. Roussis & S. Odysseos
Department of Civil and Environmental Engineering, University of Cyprus

15 WCEE
LISBOA 2012

SUMMARY:
This study investigates the effect of the impulsive nature of near-fault ground motions on the rocking response of base-isolated rigid blocks. Two models of seismic-isolation system are considered in the analysis, namely a linear model with viscoelastic behavior and a nonlinear model with hysteretic behavior. The response of the system is calculated for both recorded ground motions and simulated pulse-type motions. An extensive numerical investigation is carried out for a class of rigid blocks with different geometric characteristics, in terms of the slenderness ratio (λ) and size of the block (r), for both isolated and non-isolated blocks. The comparison of results between the rocking response of isolated and non-isolated blocks demonstrates the benefits of the isolation method: for the case of the isolated block, the initiation of rocking (uplift) is shifted towards higher values of slenderness ratio λ, while the instability region (overturning) in the λ-r space is generally reduced.

Keywords: seismic isolation, rigid block, rocking, near-fault pulse-type motions

1. INTRODUCTION

Following Housner's landmark study (Housner 1963), numerous studies (e.g. Yim et al. 1980, Ishiyama 1982, Spanos & Koh 1984, Shenton III & Jones 1991, Makris & Roussos 2000) have been reported in the literature dealing with the seismic behavior of a rigid block standing free on the horizontally-moving ground.

More recently, motivated primarily by the need to mitigate the seismic risk of objects of cultural heritage, studies on the rocking response of a rigid block with its base seismically isolated have been pursued (e.g. Vestroni & Di Cintio 2000, Caliò & Marletta 2003, Roussis et al. 2008, Contento & Di Egidio 2009, Vassiliou & Makris 2012).

This paper focuses on the nonlinear rocking response of rigid blocks free-standing on a seismically-isolated base, subjected to near-field ground motions. Near-field ground motions are typically characterized by intense velocity and displacement pulses of relatively long period that clearly distinguish them from typical far-field ground motions. The response of the system is calculated for both recorded (historic) ground motions and simulated pulse-type motions. In particular, the sophisticated analytical model of Mavroeidis & Papageorgiou (2003) has been adopted in this study in representing the near-field strong ground motions by closed-form mathematical expressions. The model adequately describes the nature of the impulsive near-fault ground motions both qualitatively and quantitatively.

The system analyzed is modeled by a rigid block standing free on a seismically-isolated base. Two models of the seismic-isolation system are considered in the analysis: (a) a linear model with viscoelastic behavior, and (b) a nonlinear model with hysteretic behavior. Upon presenting in brief the mathematical formulation of the problem (based on Roussis et al. 2008), this study focuses on an

extensive numerical investigation for a class of rigid blocks (both isolated and non-isolated) with different geometric characteristics, with the aim of investigating the effect of seismic isolation on the system dynamic behavior under near-fault ground motions, both recorded and simulated pulse-type motions.

2. ANALYTICAL MODEL

2.1. System Description

The system analyzed is modeled by a symmetric rigid block, of mass m and centroid mass moment of inertia I, standing free on a seismically-isolated base of mass m_b (Fig. 2.1). The rigid block of height $H = 2h$ and width $B = 2b$ is assumed to rotate about the corners O and O'. The distance between one corner of its base and the mass center is denoted by r and the angle measured between r and the vertical when the body is at rest is denoted by α, where $\alpha = \tan^{-1}(b / h)$. Two models of the seismic-isolation system are considered in the analysis: (a) a linear model with viscoelastic behavior, and (b) a nonlinear model with hysteretic behavior.
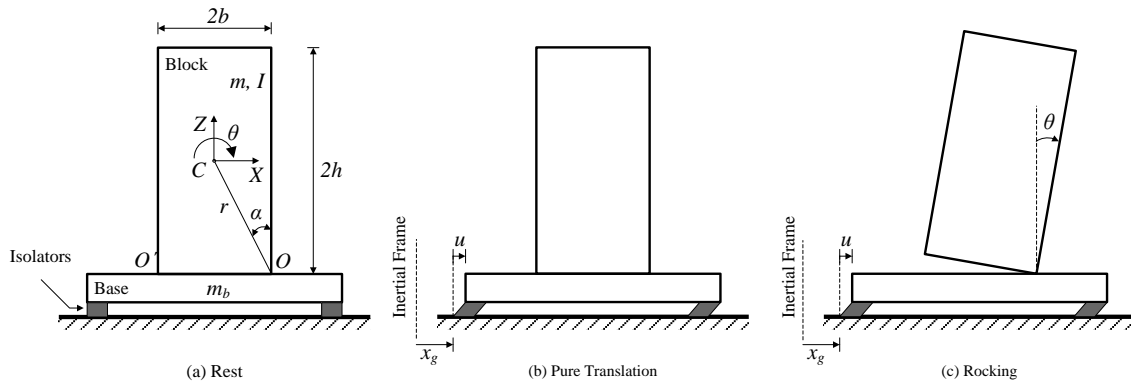
Figure 2.1. Model at rest and oscillation patterns.

The dynamic response of the system is realized through two distinct oscillation patterns; the one permitting the base-block system to translate as a whole, herein referred to as "pure translation" (Fig. 2.1b), and the other permitting the block to pivot on its edges with respect to the horizontally-moving base, referred to as "rocking" (Fig. 2.1c). Sliding of the block relative to the supporting base is not considered.

2.2. Equations of Motion

When subjected to ground acceleration $\ddot{x}_g$, the supporting base will oscillate in the horizontal direction with a displacement $u(t)$ relative to the foundation. The rigid block will be set into rocking on top of the moving base when

$$\left| \ddot{u} + \ddot{x}_g \right| > \frac{b}{h} g \tag{2.1}$$

2.2.1. Linear Isolation System

The single equation of motion of the system in the pure-translation oscillation pattern is given by

$$(m + m_b)\ddot{u} + c\dot{u} + ku = -(m + m_b)\ddot{x}_g \tag{2.2}$$

and the equations of motion of the system in the rocking oscillation pattern by

$$(m+m_b)\ddot{u}+c\dot{u}+ku+m\left[h\cos\theta+\mathrm{sgn}\,\theta(b\sin\theta)\right]\ddot{\theta}$$
$$+m\left[\mathrm{sgn}\,\theta(b\cos\theta)-h\sin\theta\right]\dot{\theta}^2=-(m+m_b)\ddot{x}_g \tag{2.3}$$

$$(mr^2+I)\ddot{\theta}+m\ddot{u}\left[h\cos\theta+\mathrm{sgn}\,\theta(b\sin\theta)\right]+mg\left(\mathrm{sgn}\,\theta(b\cos\theta)-h\sin\theta\right)$$
$$=-m\left[h\cos\theta+\mathrm{sgn}\,\theta(b\sin\theta)\right]\ddot{x}_g \tag{2.4}$$

in which $u(t)$ denotes the horizontal displacement of the base relative to the ground, $\theta(t)$ the angular rotation of the block (positive in the clockwise direction), and $\mathrm{sgn}\,\theta$ the signum function in θ.

2.2.2. Nonlinear Isolation System

The constitutive model of isolation systems modeled as elements that exhibit bilinear hysteretic behavior can be described by the Bouc-Wen model. According to this model, the restoring force in a hysteretic system is given by

$$F=K\cdot u+Q\cdot\mathbb{Z}=\alpha\cdot\frac{F_y}{Y}\cdot u+(1-\alpha)\cdot F_y\cdot\mathbb{Z} \tag{2.5}$$

where, K is the second slope of the bilinear model, Q is the strength of the system, α is the ratio of post-yield to pre-yield elastic stiffness, F_y is the yield force, Y is the yield displacement, u is the displacement, and $\mathbb{Z}$ is a hysteretic dimensional variable governed by the following differential equation:

$$Y\dot{\mathbb{Z}}+\gamma|\dot{u}|\mathbb{Z}|\mathbb{Z}|^{\eta-1}+\beta\dot{u}|\mathbb{Z}|^{\eta}-A\dot{u}=0 \tag{2.6}$$

where, A, γ, β, η are dimensionless quantities that control the shape of the hysteresis loop, with assigned values: $A=1$, $\gamma=0.9$, $\beta=0.1$, $\eta=2$, $Y=0.5$mm (Constantinou et al. 1990).

To investigate the response of isolated rigid blocks with isolation systems described by bilinear hysteretic behavior under impulsive motions, this study concentrates on the friction-pendulum system (FPS), case for which the restoring force $K=(m+m_b)g/R$ and the friction force $Q=\mu(m+m_b)g$.

Pure-translation regime

The equation of motion of the system in the pure-translation regime is given by

$$(m+m_b)\ddot{u}+Q\mathbb{Z}+Ku=-(m+m_b)\ddot{x}_g \tag{2.7}$$

which for the case of the FPS can be can be recast in the form

$$(m+m_b)\ddot{u}+\mu g(m+m_b)\mathbb{Z}+\left(((m+m_b)g)/R\right)u=-(m+m_b)\ddot{x}_g \tag{2.8}$$

Rocking regime

The set of equations of motion governing the rocking regime of the system is derived as

$$\left(m+m_b\right)\ddot{u}+Q\mathbb{Z}+Ku+m\left[h\cos\theta+\mathrm{sgn}\,\theta\left(b\sin\theta\right)\right]\ddot{\theta}$$
$$+m\left[\mathrm{sgn}\,\theta\left(b\cos\theta\right)-h\sin\theta\right]\dot{\theta}^2=-\left(m+m_b\right)\ddot{x}_g \tag{2.9}$$

$$\left(mr^2+I\right)\ddot{\theta}+m\ddot{u}\left[h\cos\theta+\mathrm{sgn}\,\theta\left(b\sin\theta\right)\right]+mg\left(\mathrm{sgn}\,\theta\left(b\cos\theta\right)-h\sin\theta\right)$$
$$=-m\left[h\cos\theta+\mathrm{sgn}\,\theta\left(b\sin\theta\right)\right]\ddot{x}_g \tag{2.10}$$

which for the case of the FPS can be can be recast in the form

$$\left(m+m_b\right)\ddot{u}+\mu g\left(m+m_b\right)\mathbb{Z}+\left(\left(\left(m+m_b\right)g\right)/R\right)u+m\left[h\cos\theta+\mathrm{sgn}\,\theta\left(b\sin\theta\right)\right]\ddot{\theta}$$
$$+m\left[\mathrm{sgn}\,\theta\left(b\cos\theta\right)-h\sin\theta\right]\dot{\theta}^2=-\left(m+m_b\right)\ddot{x}_g \tag{2.11}$$

$$\left(mr^2+I\right)\ddot{\theta}+m\ddot{u}\left[h\cos\theta+\mathrm{sgn}\,\theta\left(b\sin\theta\right)\right]+mg\left(\mathrm{sgn}\,\theta\left(b\cos\theta\right)-h\sin\theta\right)$$
$$=-m\left[h\cos\theta+\mathrm{sgn}\,\theta\left(b\sin\theta\right)\right]\ddot{x}_g \tag{2.12}$$

Evidently, the coupled equations governing the rocking regime are highly nonlinear and not amenable to closed-form solution, even for the simplest form of ground excitation. Note that Eqns (2.3), (2.4), (2.9) and (2.10) hold only in the absence of impact ($\theta\neq0$). At that instant, both corner points O and O' are in contact with the base, rendering the above formulation invalid.

2.3. Impact Model

The mathematical formulation of impact has been originally published by Roussis et al. (2008) in a paper that resolved the issue of conservation of linear momentum of the system during impact between the rocking block and its supporting base. The findings of that paper with respect to the treatment of the impact event are summarized below.

The dynamic response of the system is strongly affected by the occurrence of impact(s) between the block and the horizontally-moving base. That is, impact causes the system to switch from one oscillation pattern to another (potentially modifying the degrees of freedom), each one governed by a different set of differential equations. In addition, the integration of equations of motion governing the post-impact pattern must account for the ensuing instantaneous change of the system's velocity regime.

A model governing impact was derived from first principles using classical impact theory. According to the principle of impulse and momentum, the duration of impact is assumed short and the impulsive forces are assumed large relative to other forces in the system. Changes in position and orientation are neglected, and changes in velocity are considered instantaneous. Moreover, this model assumes a point-impact, zero coefficient of restitution (perfectly inelastic impact), impulses acting only at the impacting corner (impulses at the rotating corner are small compared to those at the impacting corner and are neglected), and sufficient friction to prevent sliding of the block during impact.

Under the assumption of perfectly inelastic impact, there are only two possible response mechanisms following impact: (a) rocking about the impacting corner when the block re-uplifts (no bouncing), or (b) pure translation when the block's rocking motion ceases after impact. The formulation of impact is divided into three phases: pre-impact, impact, and post-impact as illustrated schematically in Fig. 2.2. The impact analysis is reduced to the computation of the initial conditions for the post-impact motion, $\dot{u}^+$ and $\dot{\theta}^+$, given the position and the pre-impact velocities, $\dot{u}^-$ and $\dot{\theta}^-$.
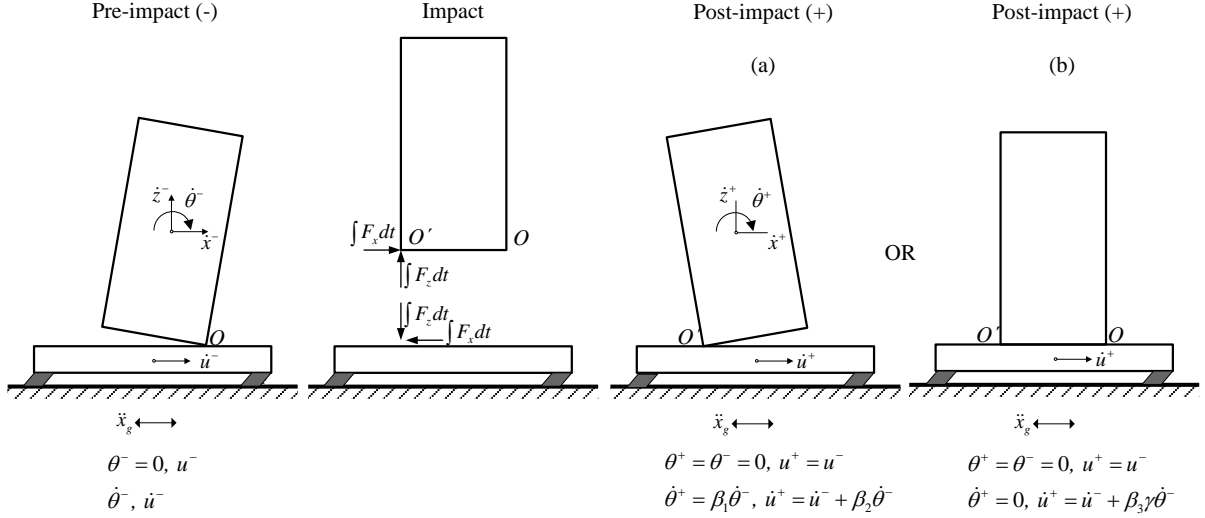
Figure 2.2. Impact from rocking about O followed by (a) re-uplift about O' and (b) termination of rocking.

In the case when the block hits the moving base from rocking about O (O') and re-uplifts pivoting about the impacting corner O' (O), the post-impact velocities in terms of their pre-impact counterparts are given by

$$\dot{\theta}^+ = \frac{\left(4m_bh^2 - 2m_bb^2 + mh^2 - 2mb^2\right)}{\left(4m_bh^2 + 4m_bb^2 + mh^2 + 4mb^2\right)}\dot{\theta}^- \tag{2.13}$$

$$\dot{u}^+ = \dot{u}^- + \frac{6mhb^2}{m_b + m}\left(\frac{m_b + m}{4m_bh^2 + 4m_bb^2 + mh^2 + 4mb^2}\right)\dot{\theta}^- \tag{2.14}$$

in which $\lambda = h/b$ is the geometric aspect ratio and $\bar{m} = m/m_b$ is the mass ratio.

In the case when rocking of the block on top of the moving base ceases, the system will attain a pure-translation regime. In this case, the post-impact translational velocity of the system, $\dot{u}^+$, in terms of the pre-impact velocities, $\dot{u}^-$ and $\dot{\theta}^-$ is given by

$$\dot{u}^+ = \frac{1}{m_b + m}\left[\left(m_b + m\right)\dot{u}^- - mh\dot{\theta}^+ + mh\dot{\theta}^-\right] \tag{2.15}$$

3. NEAR-FAULT GROUND MOTIONS

A wide range of near-fault seismic ground motions were chosen as input in the analysis of the rocking response of the system. Near-field ground motions are typically characterized by intense velocity and displacement pulses of relatively long period that clearly distinguish them from typical far-field ground motions. The response of the system is calculated for both recorded (historic) ground motions and simulated pulse-type motions. In particular, the sophisticated analytical model of Mavroeidis & Papageorgiou (2003) has been adopted in this study in representing the near-field strong ground motions by closed-form mathematical expressions. The model adequately describes the nature of the impulsive near-fault ground motions both qualitatively and quantitatively.

The mathematical representation of ground acceleration for near-fault ground motions, as proposed by Mavroeidis & Papageorgiou (2003), is

$$a(t) = \begin{cases} -\dfrac{A\pi f_p}{\gamma} \left[\begin{array}{l} \sin\left(\dfrac{2\pi f_p}{\gamma}(t-t_0)\right)\cos\left[2\pi f_p(t-t_0)+v\right] \\[2mm] +\gamma\sin\left[2\pi f_p(t-t_0)+v\right]\left[1+\cos\left(\dfrac{2\pi f_p}{\gamma}(t-t_0)\right)\right] \end{array} \right], & t_0 - \dfrac{\gamma}{2f_p} \le t \le t_0 + \dfrac{\gamma}{2f_p}, \gamma > 1 \\[6mm] 0 \end{cases} \quad (3.1)$$

where, T_p is the pulse duration, equal to the inverse of the prevailing frequency (f_p); γ is a parameter that defines the oscillatory character; A controls the amplitude of the signal; v is the phase of the amplitude-modulated harmonic; and t_0 specifies the epoch of the envelope's peak.

Table 3.1 lists the characteristics of the recorded near-fault ground motions, together with the model input parameters associated with the idealized pulses, used for the dynamic analysis.

Table 3.1. Characteristics of recorded near-fault ground motions and model input parameters for the idealized pulses (Mavroeidis and Papageorgiou (2003))

No.	Location	Station / Comp.	M_w	Dist. (km)	PGV (cm/sec)	A	γ	$v(^o)$	f_p (Hz)
1	Parkfield, CA, USA	C02/SN	6.20	0.1	75.1	60.0	1.700	100.0	0.500
2	San Fernando, CA, USA	PCD/SN	6.55	3.0	120.0	115.0	1.600	180.0	0.680
3	Bucharest, Romania	BRI/SN	7.27	190.0	74.9	62.0	2.400	200.0	0.470
4	Tabas, Iran	TAB/SP	7.11	1.2	122.0	104.0	2.200	180.0	0.190
5	Imperial Valley, CA, USA	E04/SN	6.50	6.0	78.3	71.0	1.900	305.0	0.225
		E05/SN	6.50	2.7	91.8	84.0	1.900	300.0	0.255
		E06/SN	6.50	0.3	112.0	96.0	2.100	265.0	0.260
		E07/SN	6.50	1.8	109.0	79.0	2.100	25.0	0.275
		EMO/SN	6.50	1.2	115.0	78.0	2.300	0.0	0.340
6	Northridge, CA, USA	JFA/SN	6.70	5.2	105.0	87.0	2.300	100.0	0.330
		RRS/SN	6.70	6.0	173.0	142.0	1.700	20.0	0.800
		SCG/SN	6.70	5.1	134.0	93.0	2.500	0.0	0.340
		SCH/SN	6.70	5.0	122.0	80.0	2.300	0.0	0.330
		NWS/SN	6.70	5.3	117.0	94.0	1.700	200.0	0.370
7	Aigion, Greece	AEG/Lon	6.33	6.0	40.9	44.5	1.450	75.0	1.400
		AEG/Tran	6.33	6.0	52.0	61.0	1.200	205.0	1.480
8	Izmit, Turkey	ARC/SN	7.40	14.0	44.3	41.0	1.380	225.0	0.140
		SKR/SP	7.40	3.1	80.3	67.0	1.023	5.0	0.105
		GBZ/SN	7.40	11.0	41.4	34.5	2.200	220.0	0.210
		GBZ/SP	7.40	11.0	28.7	28.0	1.800	85.0	0.165

4. NUMERICAL RESULTS

The numerical integration of the equations of motion has been pursued in Matlab (MathWorks 2006) through a state-space formulation. The computer program calculates numerically the response of an isolated block subjected to ground excitation under general conditions, considering the different possible oscillation patterns, impact, and arbitrary excitation. In particular, at each time step the program determines the correct oscillation pattern and integrates the corresponding exact highly nonlinear equations of motion. In each time step, close attention is paid to the possibility of transition

from one pattern of motion to another and to the accurate evaluation of the initial conditions for the next pattern of oscillation, on the basis of the developed impact model.

This section presents an extensive numerical investigation for a class of rigid blocks (both isolated and non-isolated) with different geometric characteristics, in terms of the slenderness ratio (λ) and size (half-diameter) of the block (r), with the aim of investigating the effect of seismic isolation on the system dynamic behavior under near-fault ground motions, both recorded and simulated pulse-type motions (Table 3.1). Two models of the seismic-isolation system are considered in the analysis: (a) a linear model with viscoelastic behavior, and (b) a nonlinear model with hysteretic behavior.

Figs. 4.1 through 4.4 report results in the form of behavior maps for a wide range of isolated and non-isolated rigid blocks under recorded near-fault ground motions. A total of 2,440 nonlinear dynamic analyses were performed in constructing each behavior map. Each dot in these maps represents the outcome of a single analysis. The blue circles indicate "No Rocking", the green "Rocking", and the red circles "Overturning" of the block. The comparison between the two maps reveals the benefits of the isolation method. Evidently, for the case of the isolated block, the initiation of rocking (boundary between the blue and green areas) is shifted towards higher values of slenderness ratio λ and the instability region (indicated in red) is generally reduced.
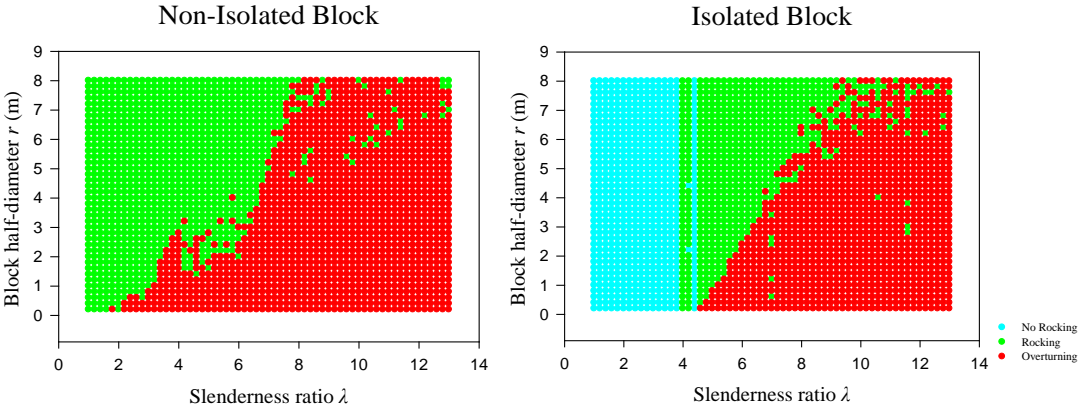
Figure 4.1. Behavior maps for a class of rigid blocks under the SN component of 1971 San Fernando, CA earthquake ($\overline{m} = 0.5$, $T_s = 2$ s, $\xi = 35\%$).
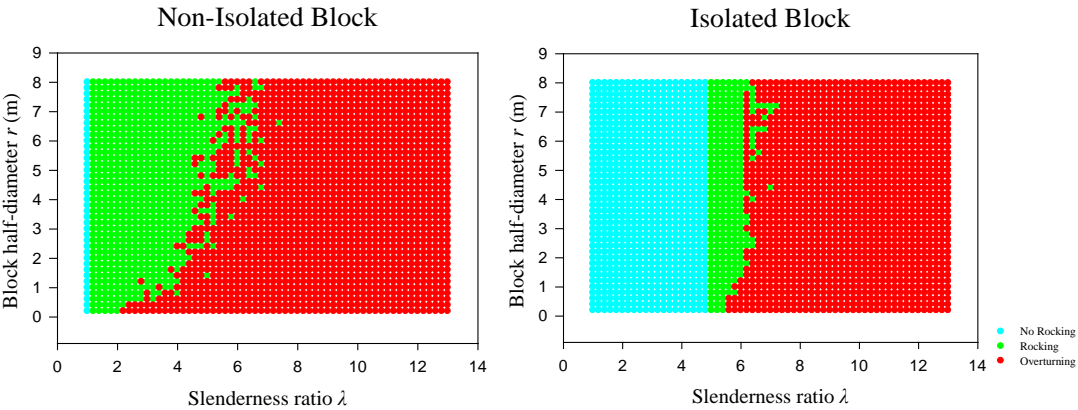
Figure 4.2. Behavior maps for a class of rigid blocks under the SP component of 1978 Tabas, Iran earthquake ($\overline{m} = 0.5$, $T_s = 2$ s, $\xi = 35\%$).
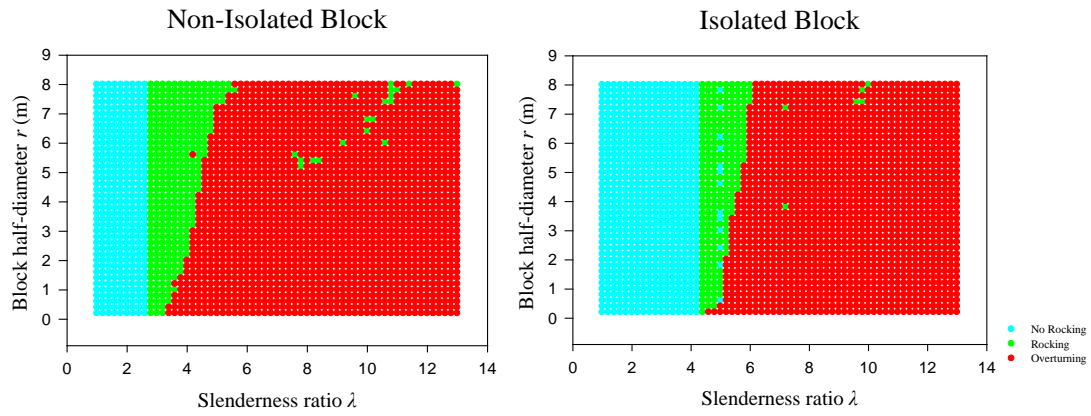
Figure 4.3. Behavior maps for a class of rigid blocks under the SN component of 1979 Imperial Valley E05 earthquake ($\bar{m} = 0.5$, $T_s = 2$ s, $\xi = 35\%$).
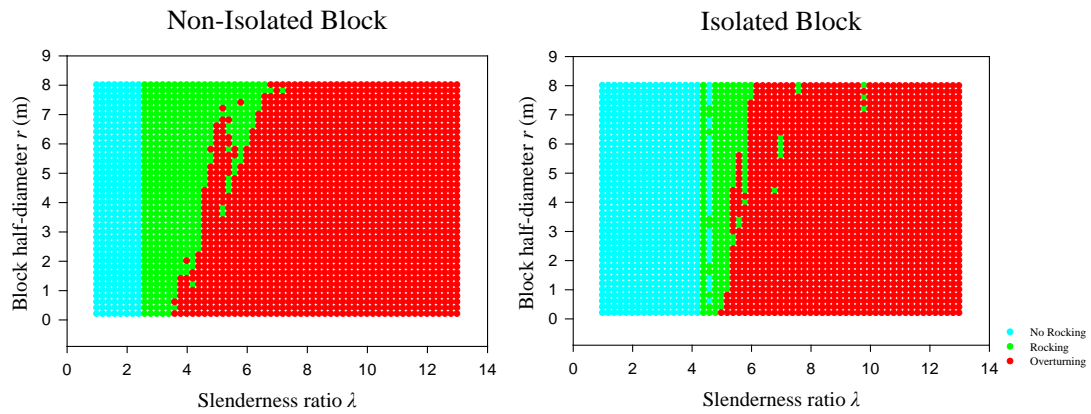
Figure 4.4. Behavior maps for a class of rigid blocks under the SN component of 1994 Northridge, CA, JFA earthquake ($\bar{m} = 0.5$, $T_s = 2$ s, $\xi = 35\%$).

Fig. 4.5 reports results in the form of behavior maps for a wide range of rigid blocks on linear and nonlinear isolation systems under the SN component of 1994 Northridge, CA, JFA earthquake. As demonstrated in these maps, the dynamic behavior of the block for the two types of seismic isolation is similar, with the initiation of rocking (boundary between the blue and green areas) not affected.
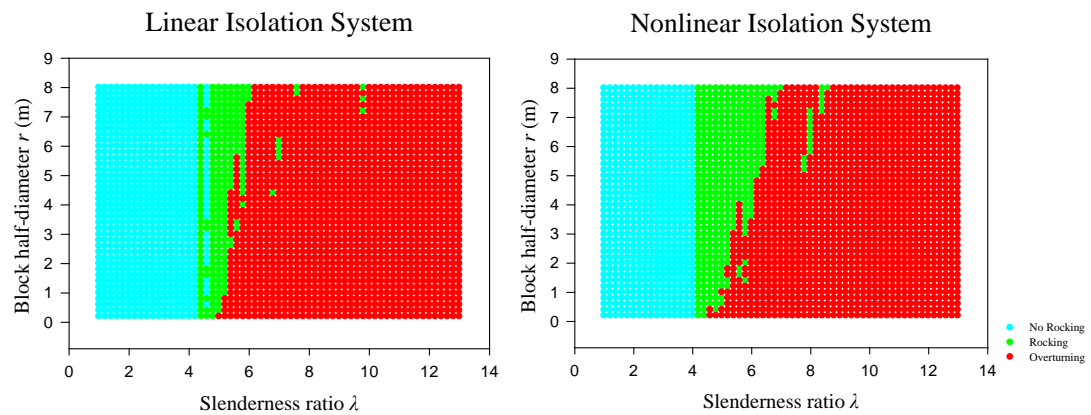
Figure 4.5. Behavior maps for a class of rigid blocks under the SN component of 1994 Northridge, CA, JFA earthquake ($\bar{m} = 0.5$, $T_s = 2$ s, $\xi = 35\%$, $\mu = 0.11$, $R = 2.24$ m).

Fig. 4.6 presents results from the dynamic behavior of isolated rigid blocks under the SN component of 1977 Bucharest, Romania earthquake and its pulse-type idealization. As seen from the ground acceleration time histories, the ground-motion model adequately describes the nature of the impulsive near-fault ground motions both qualitatively and quantitatively. Evidently, the response of the system under the recorded and simulated ground motions is comparable.
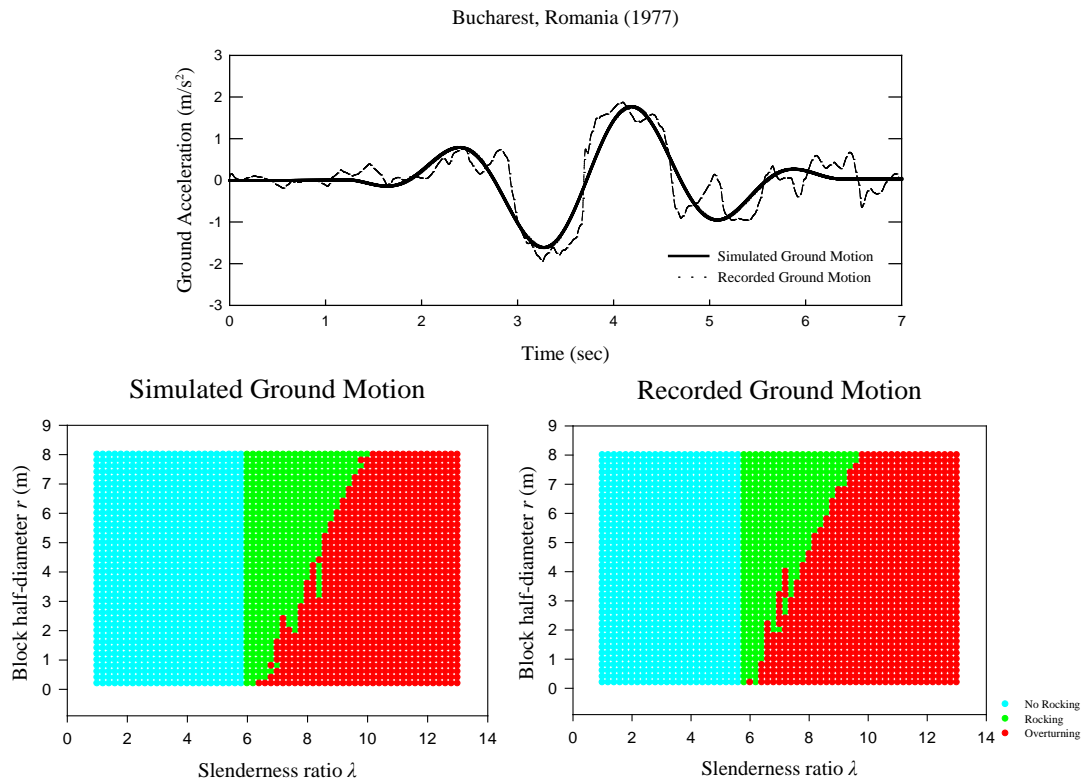
Figure 4.6. Behavior maps for a class of rigid blocks under the SN component of 1977 Bucharest, Romania earthquake and its pulse-type representation ($\bar{m} = 0.5$, $T_s = 2$ s, $\xi = 35\%$).

5. CONCLUSIONS

This study investigates the effect of the impulsive nature of near-fault ground motions on the rocking response of base-isolated free-standing rigid blocks. The response of the system is calculated for both recorded (historic) ground motions and simulated pulse-type motions. An extensive numerical investigation is carried out for a class of rigid blocks with different geometric characteristics, in terms of the slenderness ratio (λ) and size (half-diameter) of the block (r), for both isolated and non-isolated blocks. Two models of the seismic-isolation system are considered in the analysis, namely a linear model with viscoelastic behavior and a nonlinear model with hysteretic behavior.

The comparison of results between the rocking response of the two cases (isolated and non-isolated block) demonstrates the benefits of the isolation method: for the case of the isolated block, the initiation of rocking (uplift) is shifted towards higher values of slenderness ratio λ, while the instability region (overturning) in the λ-r space is generally reduced.

REFERENCES

Caliò, I. & Marletta, M. (2003). Passive control of the seismic rocking response of art objects. *Engineering Structures*, **25**, 1009–1018.

Constantinou, M.C., Mokha, A. & Reinhorn, A.M. (1990). Teflon bearings in base isolation II: Modeling. *Journal of Structural Engineering*, **116:2**, 455–474.

Contento, A. & Di Egidio, A. (2009). Base isolation of slide-rocking non-symmetric rigid blocks under impulsive and seismic excitations. *Engineering Structures*, **31**, 2723–2734.

Housner, G.W. (1963). The behavior of inverted pendulum structures during earthquakes. *GSW Bulletin of the Seismological Society of America*, **53:2**, 403–417.

Ishiyama, Y. (1982). Motions of rigid bodies and criteria for overturning by earthquake excitations. *Earthquake Engineering and Structural Dynamics*, **10**, 635–650.

Makris, N. & Roussos, Y.S. (2000). Rocking response of rigid blocks under near-source ground motions. *Géotechnique*, **50:3**, 243–262.

MathWorks (2006). Matlab: The language of technical computing, The MathWorks, Inc.

Mavroeidis, G.P. & Papageorgiou, A.S. (2003). A Mathematical Representation of Near-Fault Ground Motions. *Bulletin of the Seismological Society of America*, **93:3**, 1099–1131.

Roussis, P.C., Pavlou, E.A. & Pisiara, E.C. (2008). Base-isolation technology for earthquake protection of art objects. *In The 14th World Conference on Earthquake Engineering*. Beijing, China.

Shenton III, H.W. & Jones, N.P. (1991). Base excitation of rigid bodies. I: Formulation. *Journal of Engineering Mechanics (ASCE)*, **117:10**, 2286–2306.

Spanos, P.D. & Koh, A.-S. (1984). Rocking of rigid blocks due to harmonic shaking. *Journal of Engineering Mechanics (ASCE)*, **110:11**, 1627–1642.

Vassiliou, M.F. & Makris, N. (2012). Analysis of the rocking response of rigid blocks standing free on a seismically isolated base. *Earthquake Engineering & Structural Dynamics*, **41:2**, 177–196.

Vestroni, F. & Di Cintio, S. (2000). Base isolation for seismic protection of statues. *12th World Conference on Earthquake Engineering*.

Yim, C.-S., Chopra, A.K. & Penzien, J. (1980). Rocking response of rigid blocks to earthquakes. *Earthquake Engineering and Structural Dynamics*, **8:6**, 565–587.